Journal of Electronic Materials (2023) 52:6308–6315
https://doi.org/10.1007/s11664-023-10569-6

ORIGINAL RESEARCH ARTICLE

Characterization of Mössbauer and Superparamagnetic Properties in Maghemite Nanoparticles Synthesized by a Sol–Gel Method

Sung Yong An[1,2]

Received: 6 March 2023 / Accepted: 20 June 2023 / Published online: 11 July 2023

Abstract

Maghemite (γ-Fe_2O_3) nanoparticles were synthesized via a sol–gel process with ($Fe(NO_3)_3$ $9H_2O$) as a starting material and annealed in an Ar/H_2 (5%) balanced gas atmosphere. According to x-ray analysis, the average particle size was found to be 7.0 nm with a narrow size distribution for samples annealed at 150°C. Transmission electron microscopy (TEM) analysis also confirmed a particle size of 7.2 nm. The structural and magnetic properties were analyzed using x-ray diffraction (XRD), vibrating-sample magnetometry (VSM), and Mössbauer spectroscopy, and were found to have a spinel structure and exhibit superparamagnetic behavior. TEM was carried out to monitor the size and morphology of the particles. The hyperfine fields at 4.2 K for the *A* and *B* sites were determined to be 509 kOe and 476 kOe, respectively. The isomer shift values were $\delta_B = 0.36$ mm/s and $\delta_A = 0.32$ mm/s, which both correspond to Fe^{3+}. Since magnetite (Fe_3O_4) has Fe^{2+} and maghemite has only Fe^{3+}, it can be seen from the Mössbauer result that the powder heat-treated at 150°C is maghemite. The blocking temperature (T_B) of the superparamagnetic maghemite nanoparticles was approximately 167 ± 5 K. The magnetic anisotropy constant was calculated to be 1.4×10^6 ergs/cm^3. The coercivity value at 0 K was calculated as $H_{CO} = 174.5$ Oe.

Keywords Fe Mössbauer spectroscopy · iron oxide nanoparticles · sol–gel method · maghemite · magnetite · superparamagnetism

Introduction

Nanotechnology is a rapidly growing field of technology that has the potential to revolutionize various industries. It involves the manipulation of materials at the atomic or molecular level in order to change or enhance their properties, and to create new materials with unique physical properties. This technology has numerous applications in fields such as medicine, biology, environment, and information technology, and has led to the development of new and innovative technologies.[1–3] In particular, research in nano-biotechnology has been focused on developing diagnostic methods and treatments for diseases. By taking into account both the basic physical properties and applicability of the materials used, this field has the potential to lead to significant advances in medicine. One of the most promising applications of nanotechnology is the development of drug delivery systems and hyperthermia using magnetic nanoparticles.[4–7] To attain this goal, it is imperative to investigate the magnetic properties and medical applications of nanoscale magnetic particles. Nanoparticles that exhibit superparamagnetism have a wide range of biomedical applications, such as hyperthermia for killing cancer cells by generating heat only in cancer cells, drug delivery systems, and as contrast agents for nuclear magnetic resonance imaging. Iron oxide, due to its chemical stability and low cost, is a popular material for such studies, both domestically and internationally. Among iron oxides, maghemite (γ-Fe_2O_3) has garnered much attention for its potential applications in biomedicine.[8–11]

The sol–gel method offers significant advantages due to its chemical solution-based ambient pressure and relatively low-temperature process, making it highly suitable for large-scale applications. It allows for the precise mixing of materials at the molecular level and enables the production of nano-sized ultrafine powders with exceptional homogeneity and controlled particle size. In order to obtain

✉ Sung Yong An
sung.an@stud.assist.ac.kr

1 Seoul School of Integrated Sciences and Technologies (aSSIST), 46 Ewhayeodae 2-gil, Seodaemun-gu, Seoul 03767, Republic of Korea

2 Franklin University Switzerland, Via Ponte Tresa 29, 6924 Sorengo, Switzerland

maghemite nanoparticles, a sol–gel method was employed, which is comparable to other synthetic techniques such as co-precipitation, thermal decomposition, hydrothermal synthesis, and microwave-assisted synthesis.[1,4–8,12,13] The co-precipitation method involves the precipitation of metal salts by introducing a base or precipitating agent. While it is known for its simplicity and scalability, it often leads to larger particle sizes and agglomeration. Thermal decomposition methods entail the decomposition of precursor compounds at high temperatures to form nanoparticles. This method allows for control over particle size and crystallinity, but it is time-consuming and requires careful temperature control. Hydrothermal synthesis utilizes high temperature and pressure conditions to facilitate the formation of nanoparticles. It offers a narrow particle size distribution and improved crystallinity, but necessitates specialized equipment and longer reaction times. Microwave-assisted synthesis employs microwave radiation to expedite the synthesis process, offering advantages such as rapid heating, short reaction times, and smaller particle sizes. However, optimization is critical to prevent overheating and ensure uniform heating throughout the sample. In comparison to these methods, the sol–gel method provides simplicity, versatility, and precise control over particle size and morphology. It involves the formation of a colloidal solution or gel, followed by drying and annealing steps to obtain well-dispersed maghemite nanoparticles with properties suitable for various applications.

Mössbauer spectroscopy allows for the determination of the oxidation state of iron ions, making it particularly useful for the analysis of unknown iron compounds. It provides valuable information about the chemical composition, coordination environment, and electronic structure of iron-containing materials. Additionally, Mössbauer spectroscopy offers high sensitivity and selectivity, enabling the detection and quantification of trace amounts of iron in complex samples. This technique also provides insights into the magnetic and electronic properties of iron-based materials, contributing to a better understanding of their behavior and potential applications.[14–16]

In this study the sol–gel method was used to synthesize superparamagnetic maghemite nanopowders using iron(III) nitrate nonahydrate ($Fe(NO_3)_3\ 9H_2O$) as the starting material. The powders were annealed in a balanced gas atmosphere of Ar/H_2(5%) for 3 h at low temperatures using a unique and simple annealing process. The samples were analyzed for their structural characteristics, particle size, and magnetic properties using x-ray diffraction (XRD), Mössbauer spectroscopy, and vibrating-sample magnetometry (VSM). The results of the study provide insights into the superparamagnetic properties of iron oxide nanoparticles, which could have important implications for the development of new technologies in medicine and biotechnology.

Experiments

The ultra-fine maghemite nanopowders were synthesized using the sol–gel method with $Fe(NO_3)_3\ 9H_2O$ (99.99% purity) as the starting material. The reaction was performed at 50°C for 6 h in a mixed solvent of ethanol and distilled water (6:1 ratio), followed by the addition of 1,3-propanediol, which was stirred for 1 h. The solution was then mixed with diethanolamine for another hour before adding a small amount of acetic acid and stirring for an additional 3 h to form a 0.5 M stock solution. The solution was then dried at 100°C for 72 h to form a pre-heated powder. The dried powder was heat-treated at 150°C for 3 h in an Ar/H_2 (5%) atmosphere to obtain the ultra-fine maghemite nanopowders. The crystal structure and purity of the maghemite nanopowders were characterized using x-ray diffraction (XRD) with Cu$K\alpha$ radiation on a Philips x-ray diffractometer. For transmission electron microscopy (TEM) measurements, the samples were mounted on a carbon-coated copper grid. TEM studies were carried out on a JEM 2000EXII electron microscope. The magnetic properties, including coercivity and magnetic moment, were measured by a vibrating sample magnetometer (VSM, Lake Shore 7300) under an applied magnetic field of 10 kOe. The Mössbauer spectra were recorded using an electrodynamic acceleration spectrometer at temperatures ranging from 4.2 K to room temperature, with a 40 mCi ^{57}Co source in Rh metal serving as the γ-ray source.

Results and Discussion

The x-ray diffraction (XRD) results are shown in Fig. 1. In the case of the pre-heated powder dried at 100°C, no crystal peaks were observed (Fig. 1a). However, the XRD results for the maghemite nanoparticles annealed at 150°C showed a single phase and highly crystalline structure free from impurities (Fig. 1b). The analysis of XRD intensities, recorded as a function of Bragg's 2θ over an angular range of 20° to 80°, showed no evidence of hematite phase formation. The formation of a cubic spinel structure was confirmed by analyzing the diffraction patterns using (220), (311), (222), (400), (422), (511), (440), and (620) reflection planes. The lattice constant was calculated to be 8.348 Å using the Nelson-Riley function,[17] which is nearly the same as the lattice constant of bulk maghemite (a = 8.345 Å).[18] The broadening of the reflection peak around 35.5°, which is the main peak in Fig. 1b, observed after annealing the powder at 150°C suggests the formation of very small spinel particles. The average particle

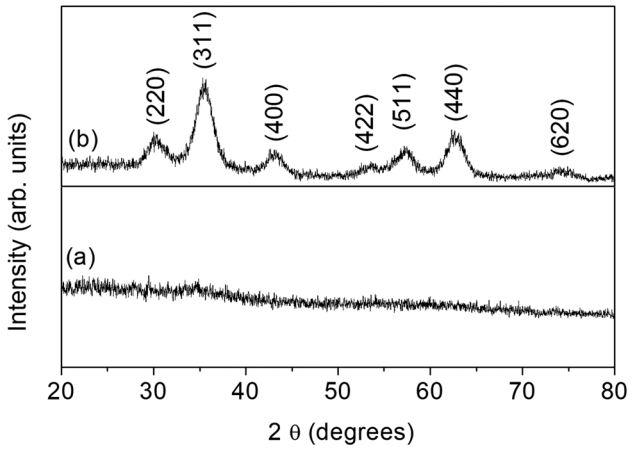

Fig. 1 XRD patterns of (a) iron oxide pre-heated powders at 100°C and (b) iron oxide nanoparticles annealed at 150°C in an atmosphere containing $Ar/H_2(5\%)$.

size was calculated using the Debye–Scherrer equation by analyzing the diffraction line width of the (311) peak.[19]

$$D_{hkl} = \frac{0.9\lambda}{\beta \cos\theta} \quad (1)$$

where 0.9 represents the Scherrer constant, λ is the wavelength of the Cu$K\alpha$ radiation ($\lambda = 1.5406$ Å), β is the broadening in the full width at half maximum (FWHM) in radians, and denotes the Bragg angle. The average particle size of maghemite calculated by the Debye–Scherrer equation was 7 nm. X-ray diffraction analysis revealed that the sample consists of a spinel structure, but it is difficult to differentiate between magnetite (Fe_3O_4) and maghemite (γ-Fe_2O_3) using XRD alone. This is because both magnetite and maghemite possess the same spinel structure, leading to almost identical positions of x-ray diffraction peaks. The differentiation between magnetite and maghemite can be made unambiguously using a Mössbauer spectrometer. The x-ray diffraction analysis of the sample dried at 100°C revealed no crystalline peaks, likely due to the low temperature inhibiting grain growth and preventing crystallization.

Transmission electron microscopy (TEM) analysis was performed to compare the particle size using the Scherrer formula. For TEM measurements, the samples were mounted on a carbon-coated copper grid. Figure 2 shows a TEM image of the 150°C annealed sample, indicating an average particle size $D \sim 7.2 \pm 0.4$ nm, with quite narrow particle size distribution. As expected, it exhibits a superparamagnetic behavior, characteristic of small magnetic particles. TEM was used for measuring the average particle size and the size distribution of those particles, defined as $D = <d\omega>/<\omega> = <dV>/<V> = <d^4>/<d^3>$, where d, ω, and V are the particle size, weight and

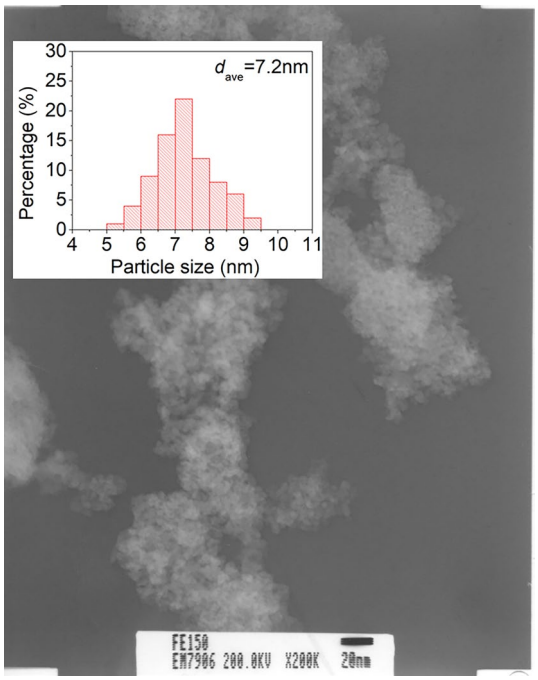

Fig. 2 TEM images of iron oxides nanoparticles annealed at 150°C in an atmosphere containing $Ar/H_2(5\%)$. The inset shows the particle size analysis (PSA) histogram and the average particle size was 7.2 nm.

volume, respectively. The results obtained from the TEM analysis showed a close agreement with the x-ray diffraction results, with both methods yielding similar particle sizes of approximately 7 nm. This consistency highlights the reliability and consistency of the particle size measurements across the different characterization techniques employed in this study. The TEM analysis revealed the presence of slight agglomeration in the nano-sized iron oxide powder and demonstrated a uniform particle size distribution. The inset in Fig. 2 presents the results obtained from particle size analysis (PSA), providing further insights into the particle characteristics. These findings highlight the importance of TEM analysis in understanding the structural properties and dispersion behavior of the iron oxide nanoparticles.

The Mössbauer spectra were measured at room temperature and 4.2 K for the pre-heated samples dried at 100°C, and the results are shown in Fig. 3 and Table I. The Mössbauer spectrum measured at room temperature of the pre-heated sample consisted of two doublets and exhibited relatively large quadrupole splitting values of 0.74 mm/s and 2.44 mm/s, and isomer shift values of 0.42 mm/s and 1.11 mm/s, which indicate the presence of Fe^{3+} and Fe^{2+} ions, respectively. As the presence of Fe^{2+} is consistent with magnetite, a Mössbauer spectrum was measured at 4.2 K to confirm this and is shown in Fig. 4. The 4.2 K

Mössbauer spectrum of the pre-heated powder, depicted in Fig. 4, also appeared as two doublets, indicating that it was not a superparamagnetic magnetite or maghemite, but rather a typical Mössbauer peak with no crystal phase. The 4.2 K spectrum also exhibited a large quadrupole splitting value and was analyzed as two doublets with Fe^{3+} and Fe^{2+} ion states. The results demonstrate that the sample dried at 100°C was still too low in temperature for crystal phase formation. For the sample heat-treated at 150°C, a single doublet was observed. A 4.2 K Mössbauer spectrum was taken to determine whether the sample was maghemite or magnetite. The 4.2 K Mössbauer spectrum showed two sextet resonance absorption lines, which were composed of two sets of *A* (tetrahedral) and *B* (octahedral) sites in a ferrimagnetic spinel structure. As shown in Table I, the ion states of both the *A* and *B* sites were Fe^{3+}, which confirms that the nanopowders heat-treated at 150°C were maghemite nanopowders. To determine whether the maghemite nanopowders have superparamagnetic properties, the Mössbauer spectrum was measured while increasing the temperature from 4.2 K to room temperature, and the Mössbauer spectra at different temperatures are shown in Fig. 5. As shown in the figure, the maghemite nanopowders with a size of 7 nm exhibit typical superparamagnetic properties. The study of superparamagnetic properties is actively pursued through Mössbauer spectroscopic experiments, which can measure small changes in specific energy using gamma-ray resonance. According to the theory of superparamagnetism,[20–22] the relaxation time of superparamagnetism, τ, can be described as

$$\tau = \tau_0 e^{(KV/K_B T)} \tag{2}$$

where τ_0 is the relaxation time constant ($\tau_0 \approx 10^{-10}$ s), K is the magnetic anisotropy constant, V is the volume of the nanoparticle, k_B is the Boltzmann constant, and T is the temperature. The resonance absorption line in the Mössbauer spectrum appears as a singlet or doublet when τ is much faster than 10^{-8} s, which corresponds to the Larmor precession time, and appears as a sharp sextet when τ is much slower than 10^{-8} s.[23] At room temperature, the resonance absorption line appeared as a doublet. However, as the temperature decreased, the area of the sextet increased and the area of the doublet decreased, as shown in Fig. 5. Below 63 K, the doublet no longer appeared in the center of the resonance absorption line. The results of the Mössbauer spectrum taken at 12 K indicate that the resonance absorption lines are composed of two sets of sextets at *A* and *B* sites, which is typical of spinel ferrite. These results suggest that the maghemite nanoparticles exhibit superparamagnetic properties at room temperature, but exhibit ferrimagnetic properties as the temperature decreases. At 4.2 K, the ultrafine magnetic field values at the *A* and *B* sites were $H_{hf}(B) = 509$ kOe and $H_{hf}(A) = 476$ kOe, and the isomer shift values were $\delta_B = 0.36$ mm/s and $\delta_A = 0.32$ mm/s, which both correspond to Fe^{3+}.

In order to confirm the superparamagnetic properties of the maghemite nanopowders, hysteresis curves were measured by applying an external magnetic field of 10 kOe at 50 K and increasing the temperature to room temperature

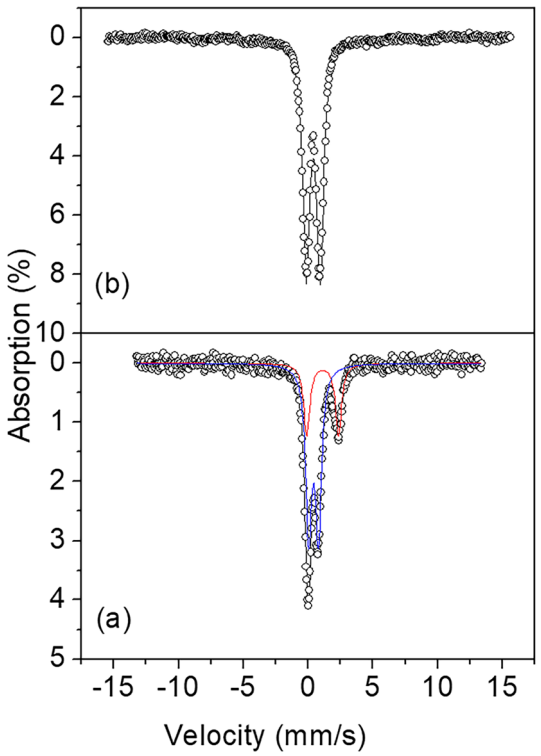

Fig. 3 Room-temperature Mössbauer spectra of (a) iron oxide pre-heated powders at 100°C and (b) iron oxide nanoparticles annealed at 150°C in an atmosphere containing Ar/H_2(5%).

Table I Hyperfine field H_{hf}, quadrupole splitting ΔE_Q, isomer shift δ for iron oxide nanoparticles annealed at 150°C and pre-heated powders measured at 4.2 K and room temperature (RT).

Sample	Iron state and site	H_{hf} (kOe)		ΔE_Q (mm/s)		δ (mm/s)	
		4.2 K	RT	4.2 K	RT	4.2 K	RT
150°C	$Fe^{3+}(B)$	508.8	–	−0.02	0.92	0.35	0.34
	$Fe^{3+}(A)$	475.8		0.04		0.31	
Pre-heated	Fe^{3+}	–	–	0.83	0.74	0.41	0.42
	Fe^{2+}	–	–	2.88	2.44	1.20	1.11

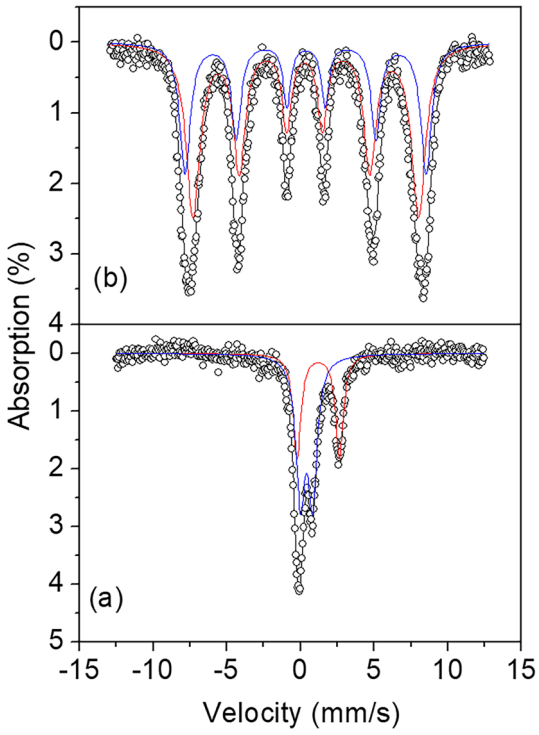

Fig. 4 Low-temperature (4.2 K) Mössbauer spectra of (a) iron oxide pre-heated powders at 100°C and (b) iron oxide nanoparticles annealed at 150°C in an atmosphere containing $Ar/H_2(5\%)$.

using a VSM. The characteristic of superparamagnetism can be confirmed through macroscopic magnetism measurements by observing that the hysteresis disappears and both the remanent magnetization (M_r) and the coercivity (H_C) are zero.[24,25] As shown in Fig. 6, the hysteresis curve measured at temperatures below 150 K displayed the characteristics of ferrimagnetism, with non-zero values for both the remanent magnetization (M_r) and the coercive force (H_C), and an increase in the coercive force as the temperature decreased. As depicted in Fig. 7a, the hysteresis curve measured at room temperature exhibited the properties of superparamagnetism, with M_r and H_C values equal to zero. This result was found to be in agreement with the results obtained from the Mössbauer experiments.

According to the theory of superparamagnetism, the magnetization of magnetic nanoparticles is free to align with the applied field when the temperature is above the blocking temperature (T_B). Below T_B, the magnetic nanoparticles exhibit ferrimagnetic behavior, as seen by the increase in remanent magnetization (M_r) and coercivity (H_C). The relative magnetization (M/M_S) curves were fitted using a log-normal Langevin function, represented by Eq. 3.[26,27]

$$f(\mu) = \frac{1}{\mu\sigma\sqrt{2\pi}} \exp\left[-\frac{\ln(\mu/\mu_0)^2}{2\sigma^2}\right] \tag{3}$$

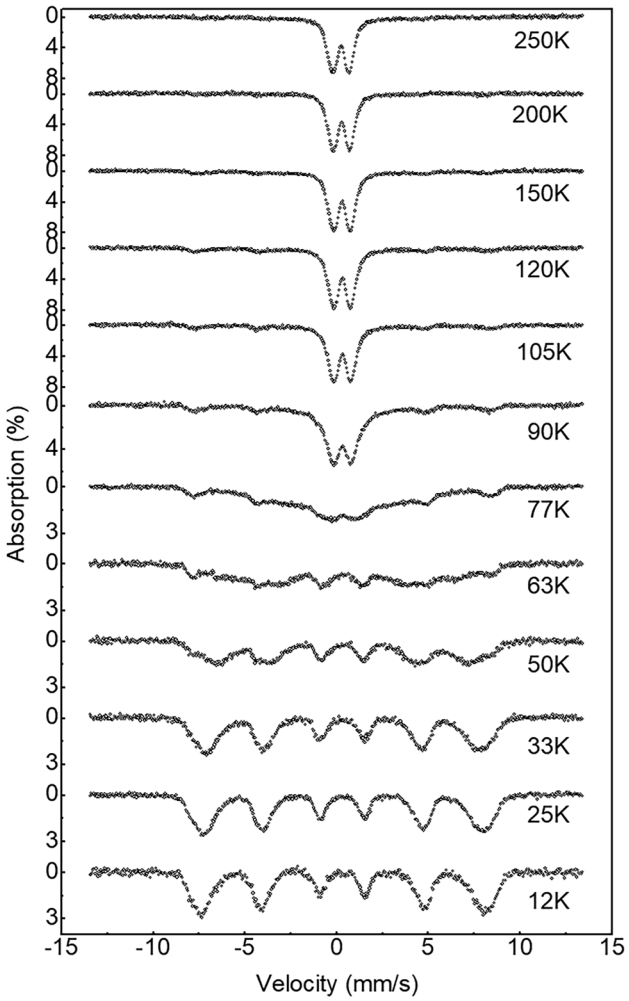

Fig. 5 Mössbauer spectra at various temperatures of maghemite nanoparticles annealed at 150°C in an atmosphere containing $Ar/H_2(5\%)$.

The function includes parameters such as the distribution width (σ) and the median of the distribution (μ_0), which is related to the average magnetic moment (μ_m).

$$\mu_m = \mu_0 \exp\left(\frac{\sigma^2}{2}\right) \tag{4}$$

The best fit based on the log-normal weighted Langevin functions was obtained with a median of the distribution $\mu_0 = 8.25 \times 10^{-17}$ emu and a distribution width $\sigma = 0.82$. Figure 7a demonstrates good agreement between the experimental and simulated relative magnetization (M/M_S) curves as a function of the external magnetic field. By assuming a log-normal size distribution of superparamagnetic particles, it was possible to calculate their particle size. This was achieved using the formula

$$\mu_m = \frac{\sigma_S \pi D^3}{6} \tag{5}$$

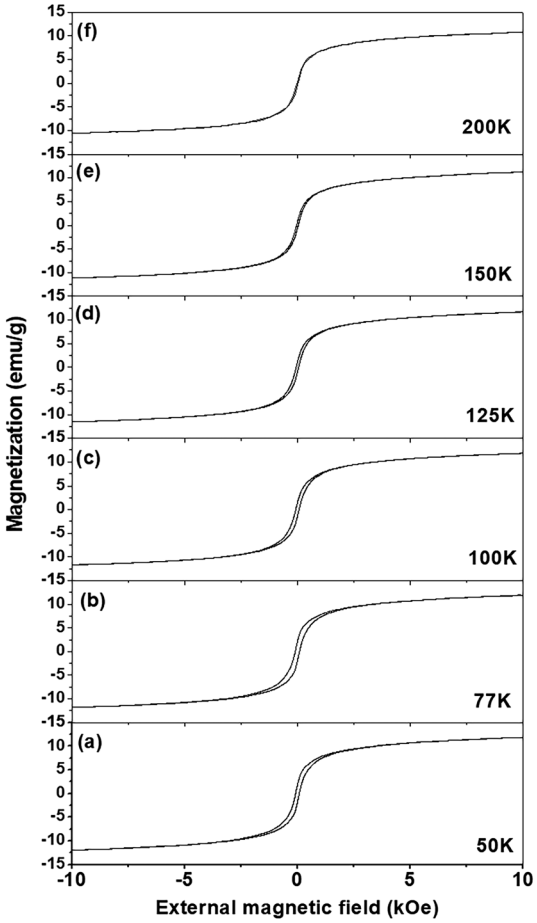

Fig. 6 Typical hysteresis loops of the maghemite nanoparticles measured at (a) 50 K, (b) 77 K, (c) 100 K, (d) 125 K, (e) 150 K, and (f) 200 K.

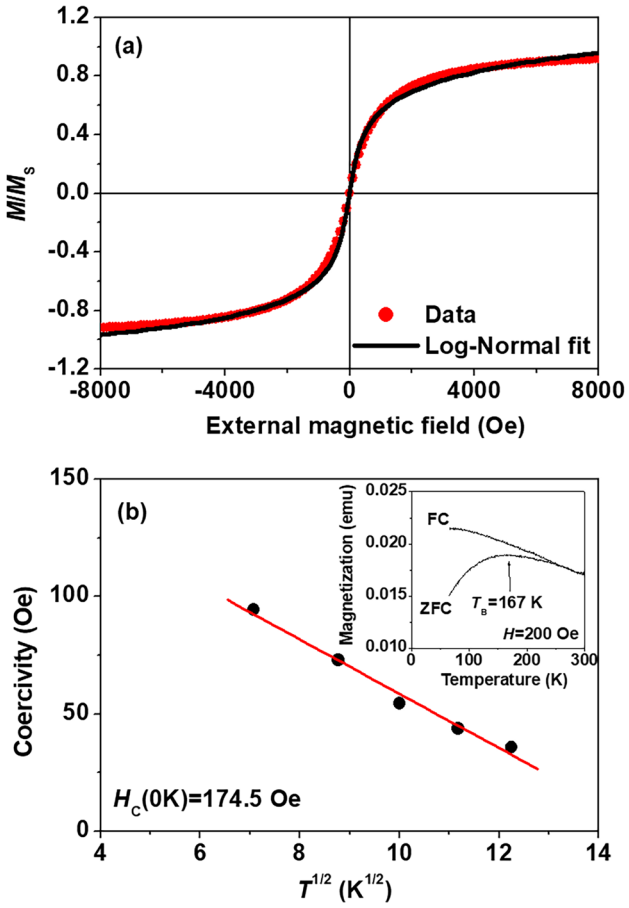

Fig. 7 (a) Experimental and calculated curves of relative magnetization as a function of external magnetic field at room temperature, (b) coercivity (H_C) plot with respect to the $T^{1/2}$. The inset shows the temperature dependence of the magnetization in the ZFC and FC cases with external magnetic field 200 Oe for maghemite nanoparticles.

where σ_s is the bulk saturation magnetization (510 emu/cm^3) and the average particle size is D, then calculated using the formula

$$D = \sqrt[3]{\frac{6 \cdot \mu_m}{\pi \cdot \sigma_S}} \tag{6}$$

The calculation of the average particle size resulted in a value of 6.8 nm, which was found to be in close agreement with the 7.0 nm obtained through the Scherrer equation. In the theory of superparamagnetism, the coercivity of the sample below the blocking temperature (T_B) has a temperature dependence described by the following equation[28–30]:

$$H_C(T) = H_{CO}\left[1 - \left(\frac{T}{T_B}\right)^{1/2}\right] \tag{7}$$

where H_{C0} is the coercivity at 0 K and T_B is the blocking temperature. Figure 7b shows the temperature-dependent coercivity, which was obtained by performing a least-squares fit. The result was a value of $H_{C0} = 174.5$ Oe. The value of the magnetic anisotropy constant K was calculated as $K = 1.4$ x 10^6 erg/cm^3 in the formula $H_{CO} = 0.64\ K/\sigma_s$. The inset in Fig. 7b shows the field-cooled (FC) and zero-field-cooled (ZFC) curves for the 7-nm maghemite nanoparticles from 65 K to 300 K at the applied magnetic field of 200 Oe. The ZFC and FC curves are coincided above 250 K and separated below 250 K. The blocking temperature was determined to be 167 K ± 5 K, which corresponded to the temperature at which the ZFC curve showed its maximum value.

Conclusion

Maghemite nanoparticles were synthesized using the sol–gel method, and the size and magnetic properties of the particles were investigated using x-ray diffraction, Mössbauer spectroscopy, and VSM. The results of the x-ray diffraction experiment indicated that heat-treating the particles

at 150°C resulted in a pure cubic spinel structure, with an average particle size of 7 nm. TEM analysis revealed slight agglomeration in the nano-sized iron oxide powder, but also indicated a uniform particle size distribution. These findings provide important insights into the structural properties and dispersion behavior of the iron oxide nanoparticles synthesized in this study. The Mössbauer spectroscopic experiment and VSM measurement showed that the heat-treated particles had superparamagnetic properties at room temperature, with a blocking temperature (T_B) of 167 K. Furthermore, the magnetic anisotropy constant (K) was determined to be 1.4×10^6 erg/cm^3. At 4.2 K, the ultrafine magnetic field values at the A and B sites were $H_{hf}(B) = 509$ kOe and $H_{hf}(A) = 476$ kOe, and the isomer shift values were $\delta_B = 0.36$ mm/s and $\delta_A = 0.32$ mm/s, which both correspond to Fe^{3+}. In conclusion, the sol–gel method is a promising method for synthesizing superparamagnetic maghemite nanoparticles with unique properties, which could be utilized in biomedicine for applications such as hyperthermia and drug delivery systems.

Acknowledgments The author would like thank Prof. Chul Sung Kim in Kookmin University for helping in Mössbauer measurements. This paper is written with support for research funding from aSSIST University.

Conflict of interest The author declares that they have no conflict of interest.

References

1. G. Kandasamy, A. Sudame, T. Luthra, K. Saini, and D. Maity, Functionalized hydrophilic superparamagnetic iron oxide nanoparticles for magnetic fluid hyperthermia application in liver cancer treatment. *ACS Omega* 3, 3991 (2018).
2. A.S. Agnihotri, A. Varghese, and M. Nidhin, Transition metal oxides in electrochemical and bio sensing: a state-of-art review. *Appl. Surf. Sci. Adv.* 4, 100072 (2021).
3. J. Palzer, L. Eckstein, I. Slabu, O. Reisen, U.P. Neumann, and A.A. Roeth, Iron oxide nanoparticle-based hyperthermia as a treatment option in various gastrointestinal malignancies. *Nanomaterials* 11, 3013 (2021).
4. J.D. Rybka, Radiosensitizing properties of magnetic hyperthermia mediated by superparamagnetic iron oxide nanoparticles (SPIONs) on human cutaneous melanoma cell lines. *Reports Pract. Oncol. Radiother.* 24, 152 (2019).
5. F. Caldera, R. Nistico, G. Magnacca, A. Matencio, Y.K. Monfared, and F. Trotta, Magnetic composites of dextrin-based carbonate nanosponges and iron oxide nanoparticles with potential application in targeted drug delivery. *Nanomaterials* 12, 754 (2022).
6. P. Hugounenq, M. Levy, D. Alloyeau, L. Lartigue, E. Dubois, V. Cabuil, C. Ricolleau, S. Roux, C. Wilhelm, F. Gazeau, and R. Bazzsi, Iron oxide monocrystalline nanoflowers for highly efficient magnetic hyperthermia. *J. Phys. Chem. C* 116, 15702 (2012).
7. S. Palanisamy and Y.M. Wang, Superparamagnetic iron oxide nanoparticulate system: synthesis, targeting, drug delivery and therapy in cancer. *Dalton Trans.* 48, 9490 (2019).
8. M. Bustamante-Torres, D. Romero-Fierro, J. Estrella-Nunez, B. Arcentales-Vera, E. Chichande-Proano, and E. Bucio, Polymeric composite of magnetite iron oxide nanoparticles and their application in biomedicine: a review. *Polymers* 14, 752 (2022).
9. M. Muzzio, J. Li, Z. Yin, L.M. Delahunty, J. Xie, and S. Sun, Monodisperse nanoparticles for catalysis and nanomedicine. *Nanoscale* 11, 18946 (2019).
10. Q.A. Pankhurst, N.T.K. Thanh, S.J. Jones, and J. Dobson, Progress in applications of magnetic nanoparticles in biomedicine. *J. Phys. D: Appl. Phys.* 42, 224001 (2009).
11. X. Lin, J. Song, X. Chen, and H. Yang, Ultrasound-activated sensitizers and applications. *Angew. Chem. Int. Ed.* 59, 14212 (2020).
12. M. Parashar, V.K. Shukla, and R. Singh, Metal oxides nanoparticles via sol–gel method: a review on synthesis, characterization and applications. *J. Mater. Sci. Mater. Electron* 31, 3729 (2020).
13. M. Benamara, N. Zahmouli, S.S. Teixeira, M.P.F. Graca, L.E. Mir, and M.A. Valente, Electrical and magnetic studies of maghemite (γ-Fe_2O_3) prepared by the Sol–Gel route. *J. Electron. Mater.* 51, 2698 (2022).
14. M. Fantauzzi, A. Pacella, D. Atzei, A. Gianfagna, G.B. Andreozzi, and A. Rossi, Combined use of X-ray photoelectron and Mössbauer spectroscopic techniques in the analytical characterization of iron oxidation state in amphibole asbestos. *Anal. Bioanal. Chem.* 396, 2889 (2010).
15. F. Grandjean and G.J. Long, Best practices and protocols in Mössbauer spectroscopy. *Chem. Mater.* 33, 3878 (2021).
16. E. Abdelhamid, S.S. Laha, A. Dixit, G.A. Nazri, O.D. Jayakumar, and B. Nadgorny, Exchange bias enhancement and magnetic proximity effect in $FeVO_4$–Fe_3O_4 nanoparticles. *J. Electron. Mater.* 48, 3297 (2019).
17. H.M.N.U.H.K. Asghar, M.K. Nawaz, R. Hussain, and Z.A. Gilani, Synthesis and characterization of praseodymium doped nickel zinc ferrites using microemulsion method. *J. Mater. Phys. Sci.* 1, 98 (2020).
18. M. Porru, M.D.P. Morales, A. Gallo-Cordova, A. Espinosa, M. Moros, F. Brero, M. Mariani, A. Lascialfari, and J.G. Ovejero, Tailoring the magnetic and structural properties of manganese/zinc doped iron oxide nanoparticles through microwaves-assisted polyol synthesis. *Nanomaterials* 12, 3304 (2022).
19. S. Yoon, Preparation and physical characterizations of superparamagnetic maghemite nanoparticles. *J. Magn.* 19, 323 (2014).
20. T. Saragi, B. Permana, A. Therigan, H.D. Sinaga, T. Maulana, and R. Risdiana, Study of magnetic properties and relaxation time of nanoparticle Fe_3O_4–SiO_2. *Materials* 15, 1573 (2022).
21. C. Caizer, Optimization study on specific loss power in superparamagnetic hyperthermia with magnetite nanoparticles for high efficiency in alternative cancer therapy. *Nanomaterials* 11, 40 (2021).
22. F.C. Fonseca, G.F. Goya, R.F. Jardim, R. Muccillo, N.L.V. Carreno, E. Longo, and R.R. Leite, Superparamagnetism and magnetic properties of Ni nanoparticles embedded in SiO_2. *Phys. Rev. B* 66, 104406 (2002).
23. T. Longo, S. Kim, A.K. Srivastava, L. Hurley, K. Ji, A.J. Viescas, N. Flint, A.C. Foucher, D. Yates, E.A. Stach, F. Bou-Abdallah, and G.G. Papaefthymiou, Micromagnetic and morphological characterization of heteropolymer human ferritin cores. *Nanoscale Adv.* 5, 208 (2023).
24. S.W. Lee and C.S. Kim, Superparamagnetic properties of nanoparticles $Ni_{0.9}Zn_{0.1}Fe_2O_4$ for biomedical applications. *J. Magn.* 10, 5 (2005).
25. H.E. Ghandoor, H.M. Zidan, M.H. Khalil, and M.I.M. Ismail, Synthesis and some physical properties of magnetite (Fe_3O_4) nanoparticles. *Int. J. Electrochem. Sci.* 7, 5734 (2012).
26. E.F. Ferrari, F.C.S.D. Silva, and M. Knobel, Influence of the distribution of magnetic moments on the magnetization and magnetoresistance in granular alloys. *Phys. Rev. B* 56, 6086 (1997).

27. M. Respaud, J.M. Broto, H. Rakoto, A.R. Fert, L. Thomas, B. Barbara, M. Verelst, E. Snoeck, P. Lecante, A. Mosset, J. Osuna, T.O. Ely, C. Amiens, and B. Chaudret, Surface effects on the magnetic properties of ultrafine cobalt particles. *Phys. Rev. B* 57, 2925 (1998).
28. J.R. Jeong, S.J. Lee, J.D. Kim, and S.C. Shin, Magnetic properties of Fe_3O_4 nanoparticles encapsulated with poly(D, L Lactide-Co-Glycolide). *IEEE Trans. Magn.* 40, 3015 (2004).
29. K. Maaz, A. Muataz, S.K. Hasanain, and M.F. Bertino, Temperature dependent coercivity and magnetization of nickel ferrite nanoparticles. *J. Magn. Magn. Mater.* 322, 2199 (2010).
30. M.E. Sadat, S.L. Budko, R.C. Ewing, H. Xu, G.M. Pauletti, D.B. Mast, and D. Shi, Effect of dipole interactions on blocking temperature and relaxation dynamics of superparamagnetic iron-oxide (Fe_3O_4) nanoparticle systems. *Materials* 16, 496 (2023).